JOURNAL OF MATERIALS SCIENCE 28 (1993) 5443–5450

The nature of amorphization in crystalline systems

V. A. PAVLOV
Institute of Metal Physics, Ural Division of Russian Academy of Sciences, 18 S. Kovalevskaya St., 620219 Ekaterinburg, Russia, Commonwealth of Independent States

The conditions of the transition from the crystalline to amorphous state and the process of amorphization of crystalline systems under cold plastic deformation have been studied. Two concepts of crystalline system amorphization are considered. Fusion and amorphization in the solid state are analysed, particularly in terms of the thermodynamics of reversible processes of the transition from the crystalline to the amorphous state. The mechanism of amorphization of a crystalline alloy is considered when it undergoes deformation or low-temperature annealing. The emphasis is on the system of Fe–B alloys.

1. Introduction

In practice, amorphous materials are produced mainly by the methods of quenching from the melt and condensation of dispersed films on a substrate. These techniques allow production of amorphous alloys in the form of thin strips and films. They are widely used in instrument making. Manufacture of bulky articles from amorphous strips proves to be a rather difficult technological operation and in many cases the quality of articles produced in this way does not satisfy engineering requirements.

These circumstances, have probably given impetus to works aimed at studying the possibilities of obtaining amorphous and ultradispersed materials by cold plastic deformation, as well as at investigating the mechanism by which crystalline systems transform to the amorphous state as a result of a solid-phase reaction.

Here an attempt is made to generalize the results of these works and to determine the pathways for further investigations.

2. Theoretical concepts

2.1. Two concepts of the nature of amorphization in crystalline systems

At present, two methods are used most widely for the production of amorphous metal systems: (1) rapid (10^6–10^8 K s^{-1}) cooling of the melt, and (2) crystalline system dispersion.

When studying the mechanism of formation of the amorphous structure in metals and alloys, one usually considers conditions of rapid quenching from the melt, because this method is employed to produce the overwhelming majority of the existing amorphous metal materials. This mechanism is essentially the solidification of an undercooled liquid. Conditions are provided, where a liquid amorphous state transforms into a solid amorphous state without the formation of crystals, due to the rapid cooling. To account for this process, a *TTT* diagram is usually plotted in temperature, T, – time, t, coordinates (Fig. 1), where T_{melt} is the melting temperature, T_n the temperature of the highest rate of formation and growth of the crystalline phase nuclei, T_g the glass transition point, and T_x the glass crystallization start temperature. The curve describes the temperature dependence of the time of crystalline phase formation in liquid and solid amorphous phases.

Fig. 1a represents the trajectory of one of the possible cooling conditions. With the conditions shown in the figure, the amorphous state will not contain the crystalline phase. At a slower rate of cooling, when curve a intersects the region of the crystalline state, the amorphous phase will have metal or alloy crystals. The number of crystals will depend on the liquid cooling rate. A decrease in the relative volume, V_c/V_0 (V_c being the crystalline phase volume and V_0 the total volume), with increasing cooling rate of the $Ni_{75}Si_8B_{17}$ alloy melt is given in Fig. 2 [1].

The amorphous state crystallization temperature, T_x, depends on the holding time. Each time, t_x, has its corresponding crystallization start temperature, T_x.

It is only natural that amorphous alloys produced by quenching from the melt should be considered to be undercooled liquids and are called metallic glasses.

By the second method, the amorphous state is achieved through precipitation of the crystalline structure subject to cooling from a vapour on a substrate. Fig. 3 shows diagrammatically the changes in the phase composition of molybdenum and tungsten as a function of the substrate temperature, T, and the structure dispersion which is characterized, in this case, by the quantity $1/d$, where d is the film thickness [2].

As the film thickness decreases, α phase and the amorphous phase, a, which are not found in the usual states of these metals, appear $T_{\alpha\to a}$ and $T_{\beta\to a}$ denote

0022–2461

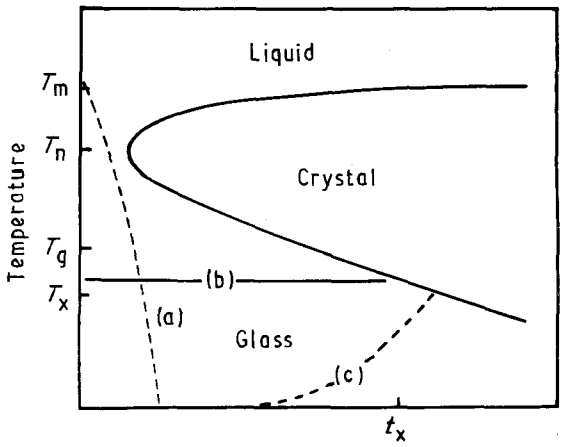

Figure 1 *TTT* diagram.

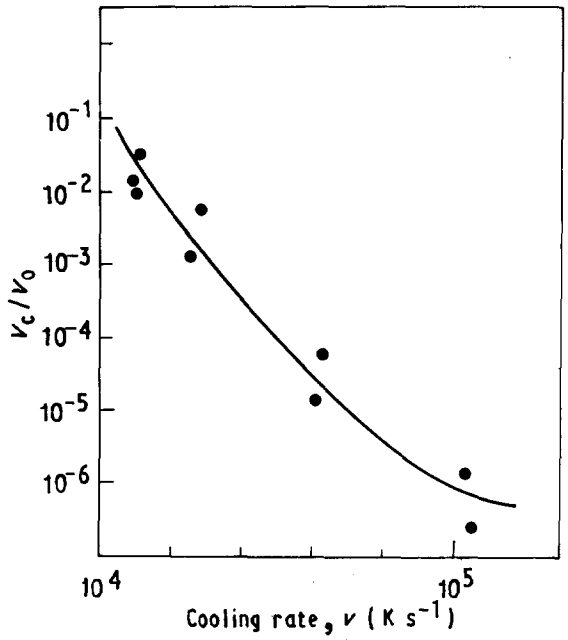

Figure 2 Dependence of the relative volume of the crystalline phase on the cooling rate of the $Ni_{75}Si_8B_{17}$ alloy [1].

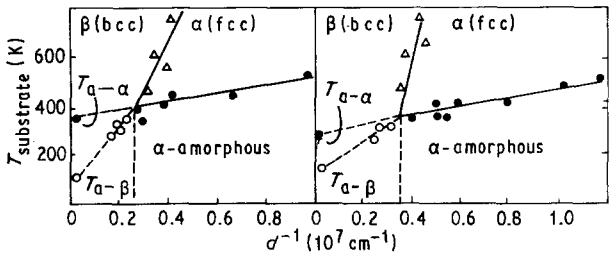

Figure 3 Phase diagrams of dispersed films of (a) molybdenum and (b) tungsten [2].

the temperatures of the phase transitions $\alpha \rightarrow$ a and $\beta \rightarrow$ a in bulky specimens if these transitions were observed in them. Each of the metastable phases, including the amorphous phase, exists over certain temperature and structure dispersion intervals. Therefore, subject to changes in thermodynamic conditions (in our case, substrate temperature, T, and/or the structure dispersion), phase transitions of the a$\rightleftharpoons\alpha$, a$\rightleftharpoons\beta$, and $\alpha\rightleftharpoons\beta$ type can, in principle, take place. In this case the amorphous state is referred to as the phase.

Whatever the nature of the metal, at temperatures $T > \frac{1}{3}T_{melt}$, condensation occurs according to the vapour $\rightarrow$ liquid reaction with subsequent crystallization, while at temperatures $T < \frac{1}{3}T_{melt}$ it occurs by the vapour $\rightarrow$ crystal mechanism [3]. In the latter case the film structure corresponds to the structure of crystalline materials which were subjected to a rather high degree of cold plastic deformation. The density of dislocations attains 10^{10}–10^{11} cm^{-2} and that of dislocation kinks is of the order of 2×10^{14} cm^{-3} [4].

2.2. Fusion and amorphization in the solid state

In order to understand how the amorphous structure is finally obtained as a result of the structure dispersion, it is expedient to turn to Frenkel's ideas formulated many years ago [5]. He considered the mechanism of transition from the crystalline to amorphous state as an example of fusion. In his opinion, the main distinctive feature of a liquid obtained by fusion of a solid is that the volume of the liquid is approximately 3% larger than the solid state of the crystal. This probably means that the interplanar spacing of the crystal lattice increases by $\sim 1\%$ by the moment of fusion. Then the crystal melts or, more precisely, goes to the amorphous state not because it becomes heated but due to an increase in its volume.

Thus, transition of a crystal to the amorphous state on fusion is a process that leads to a considerable increase in the free volume of the metal. This free volume may be distributed uniformly between all the atoms, thus leading to variations in the interplanar spacing of the crystal lattice, or may exist as separate vacancies (holes), leaving the interplanar spacing unchanged. If the free volume grows at the expense of vacancies, their number should account for $\sim 3\%$.

According to Frenkel, this mechanism of transition from the crystalline to amorphous state may take place not only on fusion, where the amorphous phase is a liquid, but also when a solid possesses an amorphous structure. Therefore the "crystal amorphous structure" phase transition can, in principle, take place at an arbitrary low temperature relative to the melting temperature, provided one ensures in some way the required increase in the free volume, such that the crystal lattice becomes unstable and relaxes to the amorphous structure as abruptly as it does on fusion.

Frenkel was probably among the first who voiced an hypothesis that the crystal amorphous structure transition can occur as a result of a solid-state reaction through an increase in the free volume.

Born [6] suggested, independently of Frenkel, a thermodynamic theory of fusion, which is based essentially on the same concepts as those used by Frenkel. As the characteristic of the lattice state, Born took the shear modulus whose magnitude tends to zero at the moment the crystal melts. He demonstrated (Fig. 4) that the relative volume, V/V_0 (V_0 being the atomic volume at $T = 0$ K) first increases linearly with T/θ

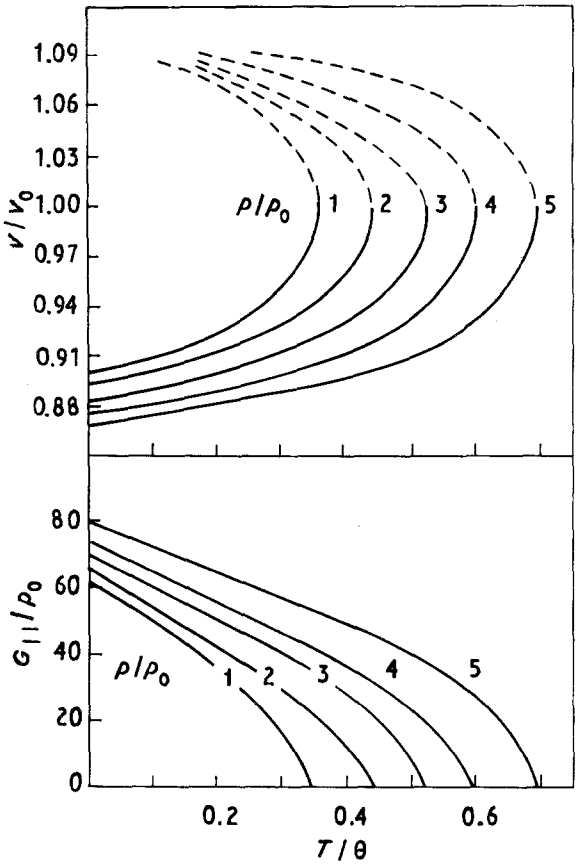

Figure 4 V/V_0 and C_{11}/p versus T/θ according to Born's [6].

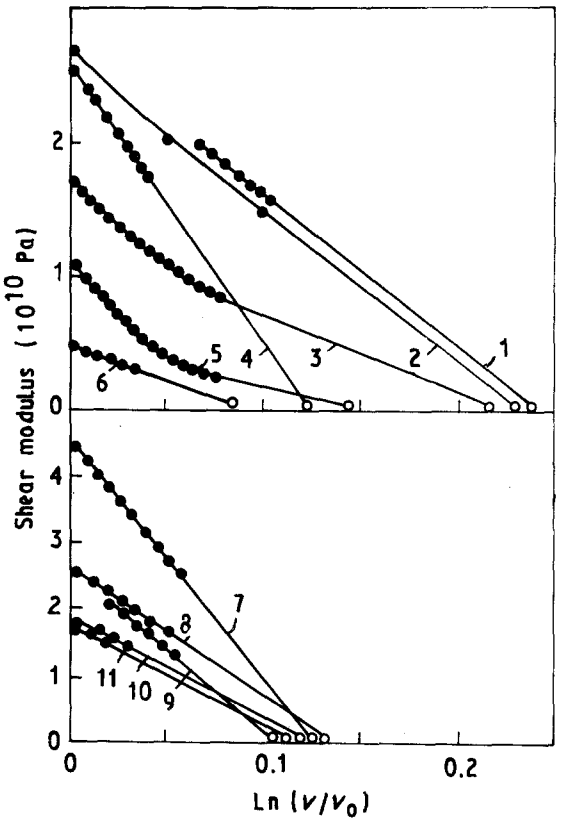

Figure 5 Shear modulus versus true change in the relative volume $\ln(V/V_0)$ [7] : 1, benzene C_{66}; 2, crypton C_{44}; 3, argon C_{44}; 4, copper $\frac{1}{2}(C_{11}-C_{12})$; 5, silver bromide $\frac{1}{2}(C_{11}-C_{12})$; 6, lead $\frac{1}{2}(C_{11}-C_{12})$; 7, zinc C_{44}; 8, aluminium $\frac{1}{2}(C_{11}-C_{12})$; 9, cadmium C_{44}; 10, silver $\frac{1}{2}(C_{11}-C_{12})$; 11, gold $\frac{1}{2}(C_{11}-C_{12})$. (●) Relative volume at the crystallization temperature and zero shear modulus.

(θ being proportional to the dissociation energy of a two-particle molecule) and then much faster, as long as the curve tends to infinity. This extreme point is the absolute limit of instability. However, the author continued these curves as dashed lines which express the region of unstable states.

Simultaneously, the shear modulus (see Fig. 4) decreases gradually and becomes zero as soon as the temperature which corresponds to the critical value of V/V_0, is achieved. This corresponds to the liquid state. As the hydrostatic pressure is increased, the crystal volume remains unchanged but the critical temperature rises.

Thus, in his theory, Born reaches the conclusion that fusion of metal systems is due to an increase in the relative volume to the critical value, at which the crystal system becomes unstable. No potential barrier is present for the transition to another state (fusion, amorphization) and fusion occurs in a catastrophic manner.

To verify Born's theory, the dependence of the shear modulus on variations in V/V_0 was studied [7]. Fig. 5 shows changes in shear moduli as a function of the true value of the volume $\ln(V/V_0)$. The values of the relative volume at the crystallization temperature and zero shear modulus are shown. The data have been obtained for a broad range of materials (metallic, ionic, molecular and organic crystals of different symmetry) and probably reflect with sufficient accuracy general regularities.

These investigations demonstrate convincingly the truth of Frenkel's and Born's hypothesis. Fusion (amorphization) indeed commences at the moment the material volume attains some critical value. The crystalline state loses stability and relaxes to the amorphous–liquid or solid state.

As follows from Figs 4 and 5, fusion (amorphization) can also take place in the solid state on condition that the necessary increase in volume is ensured.

Two very important conclusions may be drawn from the results of the theoretical and experimental investigations.

(i) It is possible, in principle, to realize the transition from the crystalline to amorphous state under the effects accompanied by the structure dispersion and an increase in the density of dislocations, disclinations, and vacancies which enlarge the crystal volume. Sufficient density of defects can be achieved under cold plastic deformation, in dispersed films, and on exposure to high-energy particles.

(ii) All the defects associated with the lattice dilatation (dislocations, disclinations, nucleating cracks, etc.) can serve as centres of the amorphous structure formation.

2.3. Thermodynamics of reversible crystal → amorphous structure transitions in the solid state

In terms of thermodynamics, the transition from the crystalline to the amorphous state can occur if the

following equations [5, 6, 8] are satisfied

$$F_c = F_a \quad (1)$$

where F_c and F_a are the free energies of the crystal and amorphous material, respectively. The free energy of the crystal can be written as

$$F_c = E_c + U_c(V) - TS \quad (2)$$

and the free energy of the amorphous state is

$$F_a = E_c + \delta E + U_c(V) + U(V) - T(S - \delta S_a) \quad (3)$$

where E_c and S are the internal energy and entropy of the crystal; $U(V)$ is the elastic energy. Then, according to Equation 1, the condition for transition from the crystalline to the amorphous state is of the form

$$U(V) = \delta E - \delta S_a T \quad (4)$$

Using known expressions for the elastic energy

$$U(V) = \frac{V_{mol}}{2} K \left(\frac{V_a - V_c}{V_c} \right)^2 \quad (5a)$$

$$V/V \approx 3(\Delta d/d) \quad (5b)$$

where V_a and V_c are the specific volumes of the amorphous and crystalline states, K the compressibility modulus, and d the lattice constant, we have

$$(9/2)V_{mol}K(\Delta d/d_0)^2 \approx \delta E - T\delta S_a \quad (6)$$

The influence of the structure dispersion on the crystal amorphous structure phase transition has been studied in detail on dispersed silicon films [8]. Fig. 6 shows the lattice constant as a function of the crystal dimension. Starting from a dimension of about 8 nm, the lattice constant grows with decreasing dimension. When the crystal dimension decreases to ~3 nm, the lattice constant increases by ~1%. The diamond lattice becomes unstable and crystalline silicon goes abruptly to the amorphous state, as it does on fusion. The X-ray diffraction pattern changes simultaneously. X-ray maxima of diffuse scattering for the amorphous state are located at other reflection angles (Fig. 7).

When silicon films are stressed, crystalline silicon transforms to the amorphous state at smaller crystal size, ~2 nm; the lattice constant varies by ~6%.

According to these data, transition of silicon from the crystalline to the amorphous state takes place on

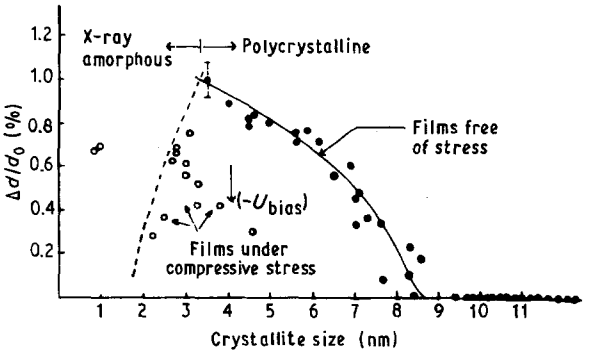

Figure 6 Correlation between the lattice dilatation $\Delta d/d_0$ and the dimension of silicon film crystals [8].

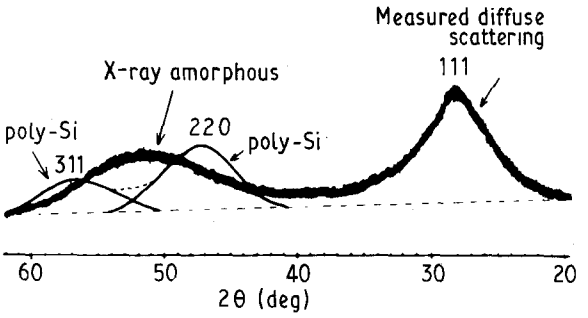

Figure 7 X-ray pattern of silicon in the amorphous state [8].

attainment of the required value of the free energy, resulting from a decrease in the crystal dimensions and a simultaneous increase of the lattice constant to critical values $(\Delta d/d_0)_{cr}$.

The authors [8] quote for silicon $\delta E \approx 0.1$–$0.6\ \mathrm{C\,mol^{-1}}$ and $\delta S \leqslant 0.4\ \mathrm{K^{-1}\,mol^{-1}}$. Using Equation 6, they obtain a value for the critical increase in the silicon lattice constant on its transition to the amorphous state at ~300 K of $(\Delta d/d_0)_{cr} \sim 0.01$–$0.02$. This value agrees well with the experimental data, Fig. 6. As mentioned above, the fine structure of dispersed films produced by condensation on a substrate at $T \leqslant \frac{1}{3}T_{melt}$ corresponds to the structure of metals with a high density of defects. Therefore, changes in the lattice constant and transition of silicon to the amorphous state are essentially due to accumulation of lattice defects – dislocations and vacancies. A considerable density of defects in a crystal lattice can be achieved if metals are irradiated with high-energy particles. The kinetics of transition to the amorphous state of GaAs was studied [9, 10] when the crystal was irradiated with Be^+ ions possessing an energy of 450 keV. The dose was $1 \times 10^{14}\ \mathrm{cm^{-2}}$. These authors came to the conclusion that the amorphous state was formed through relaxation of the crystal lattice when the critical density of vacancies was achieved. Accumulation of vacancies was accompanied by their disappearance, due to the continuous process of crystal structure restoration, and therefore the amorphous state was formed as a result of competition between these two processes. They found the critical value of the energy required for GaAs to transform to the amorphous state to be 11 ± 0.2 eV per molecule under the given conditions of irradiation.

The above experimental data refer to the case where the crystal → amorphous structure transition is due to an increase in the volume caused by defect accumulation. It might be well to consider experimental data concerning transition of the amorphous structure to the crystalline one with decreasing free volume. To illustrate this situation, let us take as an example the transition of the $Ge_{20}Te_{80}$ amorphous alloy to the crystalline state under the action of hydrostatic pressure [11]. Fig. 8a shows electrical resistivity versus hydrostatic pressure. As the pressure is raised to ~5 GPa, electrical resistivity decreases linearly. If the pressure is further increased slightly, electrical resistivity drops sharply by approximately five orders of magnitude.

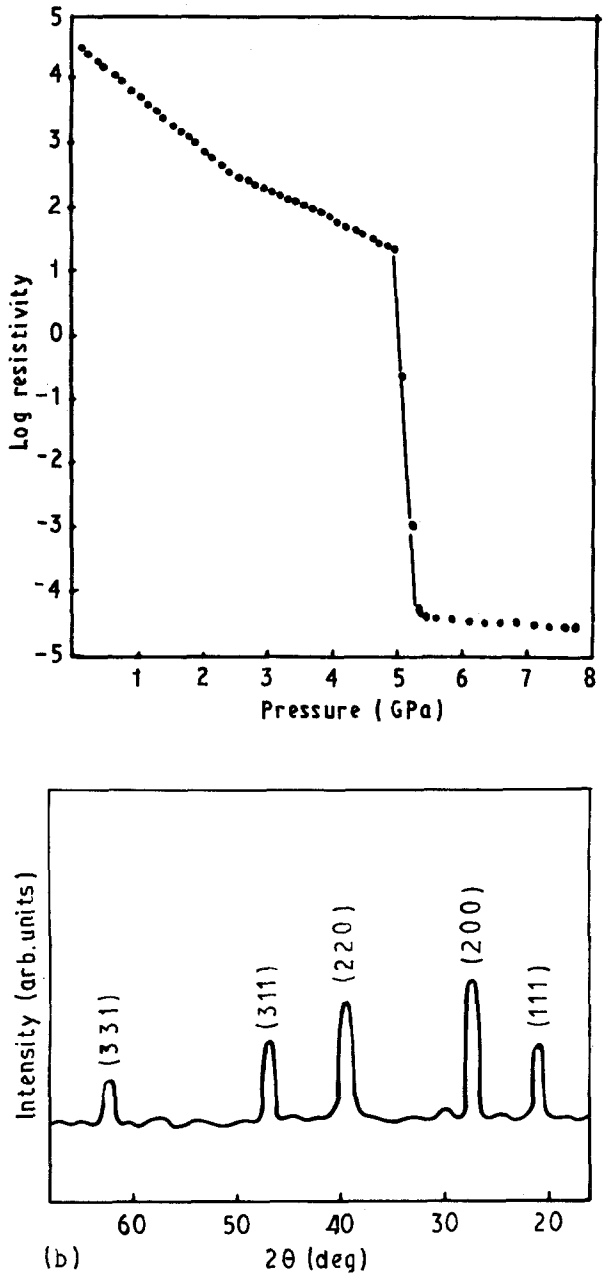

Figure 8 (a) Variations in electrical resistivity of the $Ge_{20}Te_{80}$ amorphous alloy subject to hydrostatic pressure; (b) X-ray pattern of the alloy under a 7 Gpa pressure [11].

Investigations show that this effect is connected with the phase transition of the amorphous alloy to the crystalline state with a face-centred lattice whose constant equals 0.6 nm (Fig. 8b). As soon as the hydrostatic pressure is removed, the crystal returns to the amorphous state. This is why X-ray investigations were carried out on a quenched alloy. In this case a reversible crystal → amorphous structure transition is realized on application and removal of hydrostatic pressure, with a simultaneous decrease and increase in the free volume of the alloy.

Interesting data on the reversible crystal → amorphous structure phase transition in Cr–Ti alloy subject to temperature variations are given by Blatter and Allmen [12]. The alloy was obtained as thin (150 nm) films on sapphire or tungsten. Following fusion and homogenization, the films were quenched using a laser beam. The cooling rate was (1–3) $\times 10^9$ K s^{-1}.

Fig. 9 shows diagrams of the free energy at (a) 600 and (b) 800 K for the Cr–Ti alloy depending on the titanium concentration. Changes are shown in the free energy of the metastable crystalline phase, β of the amorphous phase, a, and of the stable equilibrium crystalline phase Cr_2Ti, C_e.

Arrows indicate phase transitions on heating to 600 and 800 K. At 600 K the free energy of the metastable phase, β, is higher than the energy of the amorphous phase, a, over some interval of concentrations. As a consequence, the β-phase transforms to the amorphous state. As the temperature is raised to 800 K, the free energies of the phases change. Now the free energy of the amorphous state exceeds that of the β-phase over some concentration interval. This is accompanied by transition of the amorphous state to the metastable β-phase. Cooling of the alloy from 800 K to 600 K is followed by transition of the β-phase to the amorphous state.

The experimental data given above allow us to consider the crystal $\rightleftharpoons$ amorphous state transition as a common phase transformation which occurs in the solid state subject to variations in thermodynamic parameters P, V, T, and the structure dispersion, D. It is possible for the amorphous state to exist, just like other metastable phases, but it differs from the latter in that it does not possess crystallographic symmetry.

2.4. Amorphization of the Fe–B alloy structure under plastic deformation

Obtaining amorphous states by means of crystalline structure dispersion under cold plastic deformation is one of the most promising methods for production of bulky articles. This is why many papers dealing with investigations into high plastic deformations have been published recently in Russia and other countries.

Paul [13] reports data on the structure dispersion and amorphization under cold plastic deformation for pure metals and solid solutions, as well as for Fe–Si and Ni–Si alloys. With Fe–B alloys, Pavlov *et al.* [14] expected a more complete amorphization of the structure. As is known, in the case of alloys used for production of metallic glasses, the change in volume occurring on transition from the crystalline to the amorphous state is only 1%–2%. Fig. 10 gives an example of variations in the specific volume as a function of the boron concentration in iron for the amorphous and crystalline phases [15]. Over the range of boron concentrations which are usually used to obtain amorphous alloys, the difference in the specific volumes for the crystalline and amorphous phases is very small. Proceeding from this, one might expect that the conditions Equation 6 ensuring amorphization could be achieved in these alloys at lower degrees of deformation compared to other instances.

3. Experimental procedure

3.1. Alloys

For these investigations, alloys containing 5, 10 and 15 at % B were produced. Ingots were forged at 1100–1000 °C to bars of 15 mm diameter and were air

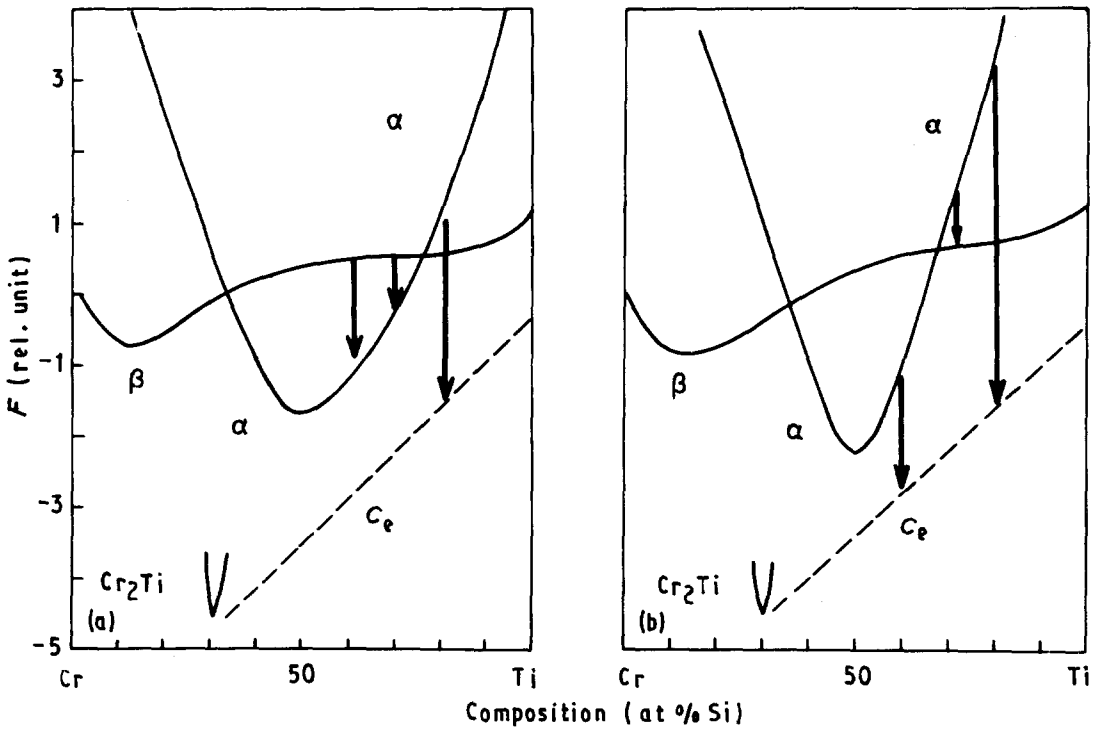

Figure 9 Phase diagram of Cr–Ti [12], (a) at 600 K, (b) at 800 K.

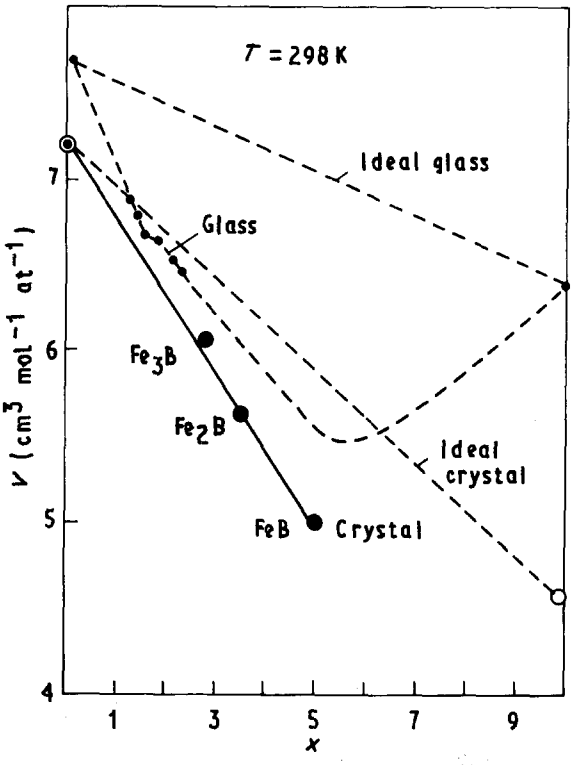

Figure 10 Molecular volume versus concentration of the $Fe_{100-x}B_x$ alloy for the crystalline and amorphous states [15].

cooled. Specimens 14 mm diameter and 100 mm long were made out of the bars for deformation tests.

3.2. Deformation

The specimens were deformed by hydrostatic extrusion at room temperature. Deformation was effected in steps of 50%, 70% and 90% ψ (ψ being a decrease in the cross-sectional area of a specimen).

3.3. X-ray analysis

X-ray analysis was performed after each deformation step. Different kinds of $Fe_{100-x}B_x$ phases could be expected to arise under plastic deformation and annealing. To provide for a more accurate determination of the alloy phase composition, X-ray patterns were taken under conditions ensuring sufficiently sharp diffraction maxima. Therefore, filtered MoK_α irradiation was used, with a slot width of 0.25 mm.

4. Results

Qualitatively similar results have been obtained for all the alloys studied. For this reason, only the data obtained on Fe–5 at % B are discussed.

Subsequent to forging, the specimen structure comprises two phases, α-Fe and Fe_2B. This state is shown in Fig. 11a. As is seen, the most intense lines are due to the α-Fe phase. X-ray lines of the Fe_2B phase are less intense.

For plastic deformation, $\psi \sim 70\%$, the following changes are observed: first, the line (1 1 2) Fe_2B disappears and, second, the intensity of the line (2 0 0) α-Fe is reduced (Fig. 11b). As deformation is increased to $\psi \sim 90\%$, these changes progress (Fig. 11c). As a result, all the X-ray lines belonging to the Fe_2B phase disappear. The intensity of the lines (2 0 0), (2 1 1) and (3 1 0) α-Fe largely decreases. The most intense lines of the α-Fe phase are (1 1 0) and (2 0 0).

Interesting data have been derived from studying the effect of annealing at 300 °C on the alloy which was deformed initially to $\psi \sim 70\%$. An X-ray pattern for a 4 h anneal is given in Fig. 12a. A comparison of the X-ray patterns in Figs 12a and 11b shows that during annealing the process of the structure variation follows the same trends as during plastic deformation. The line (2 0 0) Fe_2B vanishes and the intensity of the

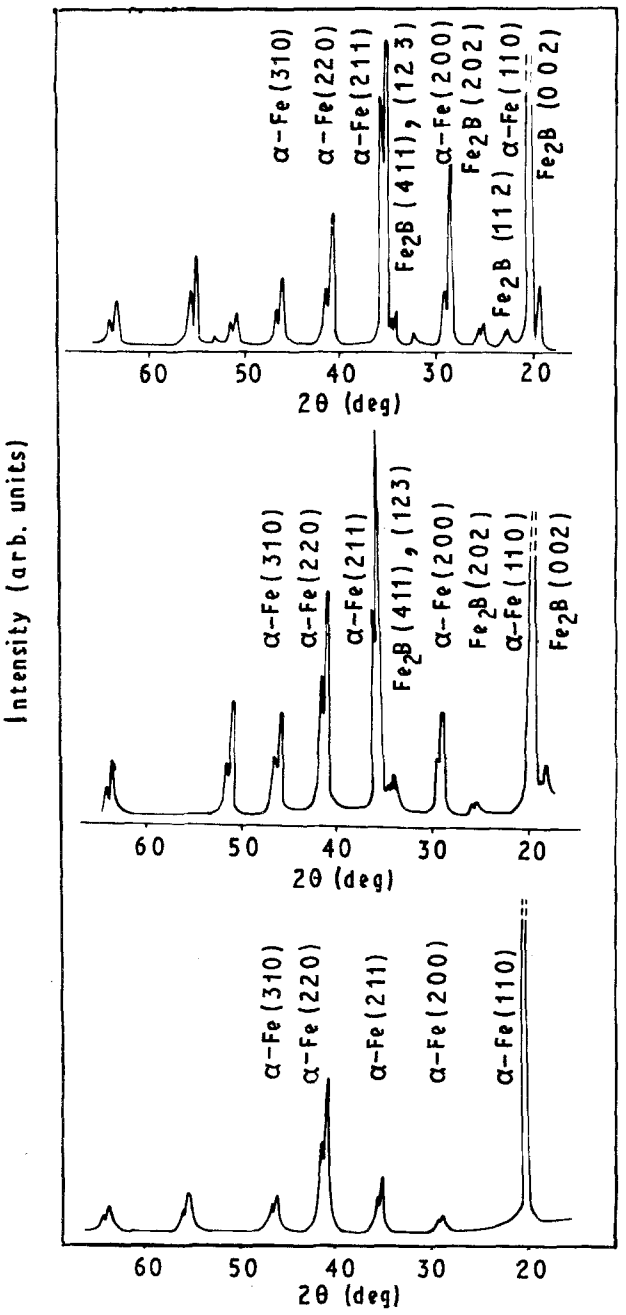

Figure 11 X-ray patterns of the Fe–5 at % B alloy, (a) after forging, (b) after additional cold deformation to $\psi \sim 70\%$, (c) after cold deformation, $\psi \sim 90\%$.

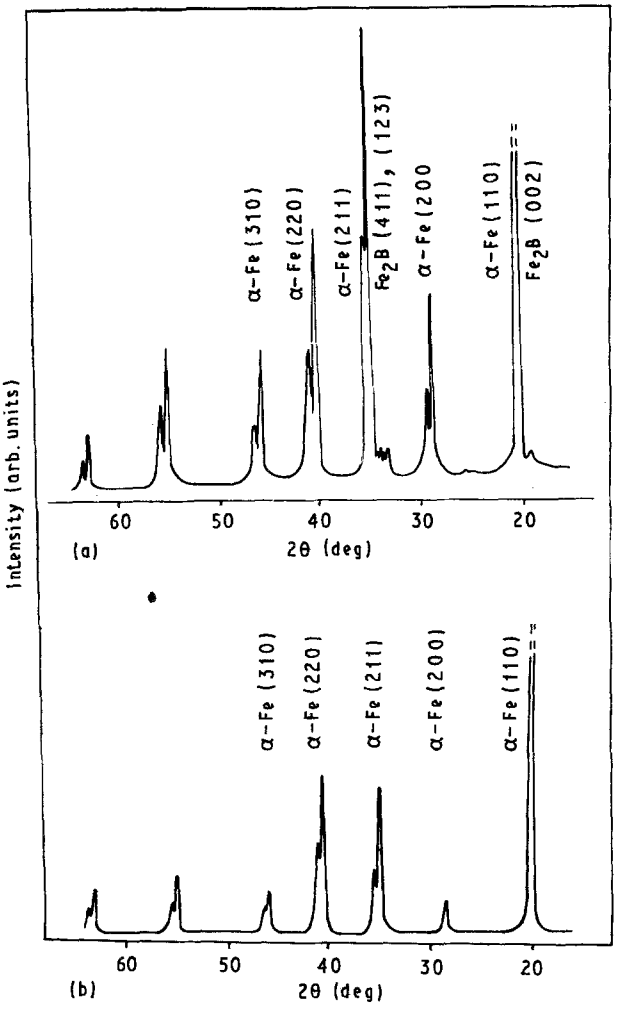

Figure 12 X-ray pattern of the Fe–5 at % B alloy: (a) preliminary cold deformation $\psi \sim 70\%$ and subsequent annealing at 300 °C for 4 h; (b) preliminary cold deformation $\psi \sim 70\%$ and subsequent annealing at 300 °C for 8 h.

line (0 0 2) Fe_2B is reduced. Much greater changes take place if the annealing time is increased to 8 h (Fig. 12b). In this case all the lines due to Fe_2B disappear. The most intense lines of α-Fe are (1 1 0), (2 1 1) and (2 2 0). This X-ray pattern is very much like its counterpart observed after a deformation $\psi \sim 90\%$ (cf. Figs 11b and 12b).

5. Discussion and conclusion

The structural changes observed during plastic deformation and low-temperature annealing point to decomposition of the Fe_2B phase and dissolution of boron in iron. However, this process cannot take place in crystalline α-Fe. This suggests that plastic deformation and low-temperature annealing performed after preliminary deformation give rise to certain processes leading to amorphization of the Fe–5 at % B alloy.

The reaction of Fe_2B decomposition and dissolution of boron proceed at anomalously high diffusion rates because the process occurs at room temperature over a short period limited by the time a unit volume is found in the deformation centre.

Considerable holding times are required for annealing at 300 °C. This is probably indicative of the fact that diffusion goes faster during deformation than during annealing.

More data are needed to explain the kinetics of the phenomenon observed. Let us try, however, to comprehend it in terms of thermodynamics. Fig. 13 presents a diagram of the free energy of an annealed Fe–B alloy comprising two phases, α-Fe and Fe_2B (curve $\psi = 0$). The same figure shows changes in the free energy under plastic deformation.

The free energy, F, of the annealed alloy is less than the energy of the amorphous state, A. Assume that for the plastic deformation ψ_1, the free energy of the deformed alloy, F_c, equals that of the amorphous state F_a, i.e. the condition

$$F_c = F_a \tag{7}$$

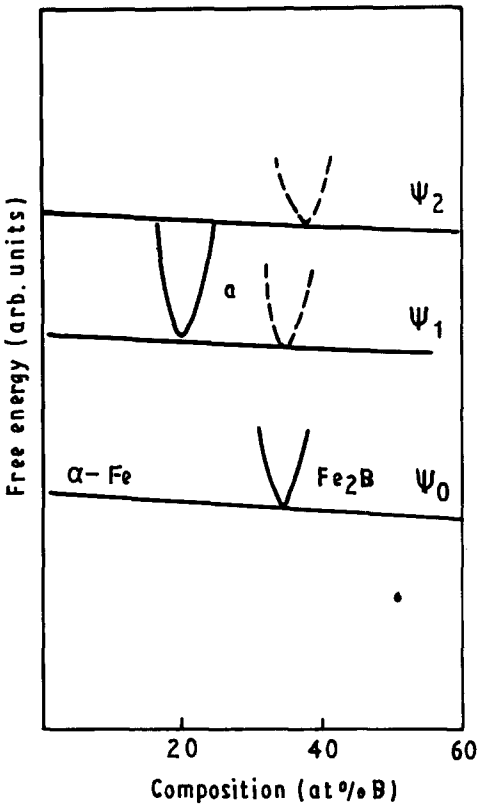

Figure 13 Variation in the free energy of the Fe–B alloy under deformation. Curve A denotes the free energy of the amorphous state.

is fulfilled. On the strength of the above concepts of the thermodynamic conditions of the crystal → amorphous structure reaction, the crystalline system should transform to the amorphous one at any temperature without thermal activation, as it does on fusion, as soon as Equation 7 is satisfied.

The process develops in this way in a homogeneous system only. In our case, however, we deal explicitly with an inhomogeneous alloy consisting of two phases, α-Fe and Fe_2B. For the crystal → amorphous structure reaction to occur, the critical condition is decomposition of the Fe_2B phase and diffusion of boron to α-Fe. Both these processes have potential barriers U_p and U_g.

The decomposition or diffusion energy imparts a thermally activated character to the process of the crystal → amorphous structure phase transition. The activation energy of the process will not be directly connected with stresses but will depend on dislocations, vacancies, and other defects [16].

Experimental investigations show that in a deformed Fe–B alloy the activation energy of the amorphization process, E, is equal to 0.2 eV [17].

References

1. D. G. MORRIS, *Acta Metall.* **31** (1983) 1478.
2. N. T. GLADKIKH and V. A. KHOTKEVICH, in "Dispergirovaniye metallich. plenok" (Izd. Akad. Nauk UkrSSR Kiev, 1972) p. 5.
3. L. S. PALATNIK, N. T. GLADKIKH and M. N. NABOKA, *Fiz. Tverd. Tela* **4** (1962) 202.
4. K. A. NEYGEBAUR, in "Fiz. Tonkikh Plenok" (Mir, Moscow, 1976).
5. Ya. I. FRENKEL, "Vvedeniye v teoriyu tverdogo tela" (Fizmatgiz, Moscow, 1958).
6. M. BORN, *J. Phys. Chem.* **7** (1939) 591.
7. J. L. TALLON, *Phil. Mag. A.* **39** (1979) 151.
8. S. VEPREK, Z. IQBAL and F.-A. SAROTT, *Phil. Mag. B* **45** (1982) 137.
9. D. K. SADANA, T. SANDS and J. WASHBURN, *Appl. Phys. Lett.* **44** (1984) 623.
10. T. SANDS, D. K. SADANA, R. GRONSKY and J. WASHBURN, *Appl. Phys. Lett.*, **44** (1984) 874.
11. G. PARTHASARATHY, A. K. BAHDYOPADHYAY, S. ASOKAN and E. S. R. COPAL, *Solid State Commun.* **51** (1984) 195.
12. A. BLATTER and M. von ALLMEN, *Phys. Rev. Lett.* **54** (1985) 2103.
13. V. A. PAVLOV, *Fiz. Met. Metalloved.* **59** (1985) 629.
14. V. A. PAVLOV, V. P. KETOVA and L. I. YAKOVENKOVA, *ibid.* **64** (1987) 940.
15. C. CUNAT, M. NOTIN and J. HERTZ, *J. Non-Cryst. Solids* **55** (1983) 45.
16. W. C. JOHNSON, *Prog. Mater. Sci.* **30** (1986) 81.
17. V. A. PAVLOV, V. P. KETOVA, N. F. VILDANOVA, V. I. SHALAEV and A. V. SHABASHOV, unpublished.

Received 26 April 1991
and accepted 1 May 1992